Indirect Vector Control of Multilevel Inverter fed Induction motor Using ANN Estimator and ANFIS Controller

Sanjaya Kumar Sahu
Dept. of Electrical Engineering
Bhilai Institute of Technology,
Durg, C.G., India
sanjayasahubit@gmail.com,

T. V. Dixit
Dept. of Elec. & Elex. Engineering
Bhilai Institute of Technology,
Durg, C.G., India
tvdixit@gmail.com

D.D. Neema
Dept. of Electrical Engineering
Chhattisgarh Institute of Technology
Rajanandgaon, C.G., India
neemadd@sify.com

***Abstract*-The indirect vector control of multilevel inverter fed three-phase induction motor using an adaptive neuro fuzzy controller and neural network estimator is proposed in this paper. The proposed scheme is realized by a three-level inverter, an adaptive neuro-fuzzy controller and two feed forward neural networks. The proposed three-level inverter is a neutral point clamped (NPC) inverter employing hysteresis current control technique for switching the IGBTs. A five layer artificial neural network (ANN) structure is used to tune the fuzzy logic algorithm in adaptive neuro-fuzzy controller. The adaptive neuro-fuzzy inference system (ANFIS) is used in place of conventional PI controller. To tune the fuzzy inference system a hybrid learning algorithm has been adopted. Two feed forward neural networks are used as estimator, learned by the Levenberg-Marquardit algorithm with data taken from PI control simulations. The performance of this scheme is investigated under various load and speed conditions. The simulation results show the suitability and robustness for high performance drive applications.**

Keyword - Multilevel Inverter, Hysteresis current control, Adaptive Neuro-Fuzzy Inference System(ANFIS), Hybrid learning algorithm, Artificial Neural Network (ANN), Back propagation algorithm, PI controller, Fuzzy logic controller(FLC).

I. INTRODUCTION

Three-phase induction motors are widely used in the industrial purpose because they show better Performance during heavy loads as well as cost effective. However the drawbacks associated with induction motor are its non-linear behavior, controllability and its complexity in developing mathematical model [1]. By vector control or field oriented control (FOC) theory, induction motor can be controlled like a separately excited dc motor. As a result field and torque of the induction machine can be controlled independently by manipulating the corresponding field oriented quantities. There are two methods of vector control - direct and indirect vector control [1]–[3]. In this paper the indirect control method is adopted, where the slip angle, the d-axis and q-axis stator currents in synchronous reference frame are computed from the torque and rotor flux and used for vector control. A multi-level inverter is a power electronic circuit built to synthesize stepped approximation of a sinusoidal wave output voltage or current from a number of DC voltages [4]. The multilevel inverters gained the attention in industrial drive application due to following features [5], [6]:

a) Improves the waveform quality as the level of inverter increases.
b) Reduces the size and rating of filter components.
c) High efficiency due to low switching frequency.
d) Lower dv/dt across switches and generate lower distorted output voltages.
e) Draw input current with very low distortion.
f) Generate smaller common-mode voltage which reduces the stress in the motor bearings.

The several multilevel inverter topologies are: The Neutral point clamped (NPC) inverter, Flying Capacitor Inverter (FCI), and Cascade H-Bridge (CHB) inverter. The NPC inverters are very popular for high voltage and high power applications. Theoretically, NPC topology with any number of levels can be realized. But some of the problems like complexity of switching algorithm, voltage unbalance across capacitors, voltage clamping requirements, and circuit layouts have limits on the level in practical multilevel inverters [7], [8].

In an N-level NPC, each phase leg consists of 2(N-1) power switches, $(N\text{-}1)\times(N\text{-}2)$ clamping diodes. The DC bus requires (N-1) bulk capacitors. The line voltage has (2N-1) Levels. At any given time there are (N-1) switches in each leg which are in ON state. Voltage rating of each of the device is assumed to be $\left(Vdc/(N-1)\right)$.

For complex, non-linear and uncertain process the fuzzy logic control has been proven as an effective solution. It deals with problems that have uncertainty and vagueness. If available data is not reliable or system is too complex to derive the required data and decision rules then the expert knowledge can be used to form proper set of rules. These set of rules are used to tune the controller for better results. Artificial Neural Network has the powerful capability for learning, adaptation, robustness and rapidity. Therefore, the advantages of Artificial Neural Network have been used for framing the proper rules of the fuzzy logic controller by adaptation and learning algorithm which is called ANFIS controller. This paper presents a scheme of Indirect vector control of multilevel inverter fed Induction motor with ANN

estimator and an ANFIS controller for improving the transient response, when it is subjected to torque and speed disturbances. The required data for training the ANN estimator and ANFIS controller is obtained by simulation of the closed loop system with PI controller.

II. MODELING

A. *Induction Motor*

The three-phase squirrel cage induction motor mathematical equations in synchronous rotating reference frames are as follows [1]–[3]:

$$V_{ds}^{e} = R_s i_{ds}^{e} + p\lambda_{ds}^{e} - \omega_e \lambda_{qs}^{e} \quad (1)$$

$$V_{qs}^{e} = R_s i_{qs}^{e} + p\lambda_{qs}^{e} + \omega_e \lambda_{ds}^{e} \quad (2)$$

$$0 = R_r i_{dr}^{e} + p\lambda_{dr}^{e} - (\omega_e - \omega_r)\lambda_{qr}^{e} \quad (3)$$

$$0 = R_r i_{qr}^{e} + p\lambda_{qr}^{e} - (w_e - w_r)\lambda_{dr}^{e} \quad (4)$$

Where,

$$\lambda_{ds}^{e} = L_s i_{ds}^{e} + L_m i_{dr}^{e} \quad (5)$$

$$\lambda_{qs}^{e} = L_s i_{qs}^{e} + L_m i_{qr}^{e} \quad (6)$$

$$\lambda_{dr}^{e} = L_r i_{dr}^{e} + L_m i_{ds}^{e} \quad (7)$$

$$\lambda_{qr}^{e} = L_r i_{qr}^{e} + L_m i_{qs}^{e} \quad (8)$$

And electromagnetic torque

$$T_e = \frac{3}{2}\frac{P}{2} L_m (i_{qs}^{e} i_{dr}^{e} - i_{ds}^{e} i_{qr}^{e}) \quad (9)$$

$$w_r = \frac{d\theta_r}{dt} \quad (10)$$

$$T_e = j_m \frac{dw_r}{dt} + B_m w_r + T_l \quad (11)$$

B. *Three-Level NPC Inverter*

The three-level NPC inverter with two DC link capacitors C_1 and C_2 in series and a neutral point 'O' is shown in Fig.1. Each phase of the three-level NPC inverter has two pair of switching device S_{i1}, S_{i2} and S_{i3},S_{i4} in series, where i = *a*, *b*, *c* phases. The center of each pair is clamped to the neutral of the DC link capacitors through the clamping diodes D_1, D_2, D_3, D_4, D_5 and D_6 [9], [10]. Table I enumerates the switching states for the semiconductor devices for the i^{th}-phase of this inverter. In Table I, the switching symbols +, 0 and - respectively denote that the i^{th}-phase terminal is connected to the positive bus, the neutral point and the negative bus.

Table 1: Switching Levels in a Three-Level NPC Inverter

S_{i1}	S_{i2}	S_{i3}	S_{i4}	i^{th} Pole voltage V_{io}
ON	ON	OFF	OFF	$V_{dc}/2$
OFF	ON	ON	OFF	0
OFF	OFF	ON	ON	$-V_{dc}/2$

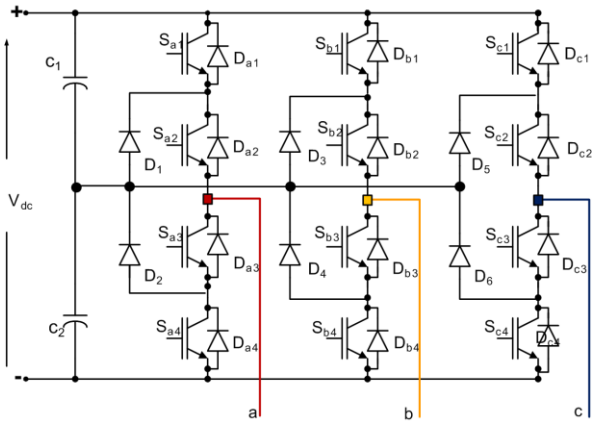

Fig. 1: Three Level NPC Inverter

C. *Three-Level Hysteresis Current Controller*

An analytical solution of different multilevel PWM techniques for three-level NPC has been presented [9], [11]. Among these techniques, the hysteresis band is used very often because of its simplicity of implementation, fast response current and robust structure [12], [13]. Hysteresis band controller is used to track the line current references. The current errors between the reference and measured currents are used to develop three valid switching states in each inverter leg by the hysteresis band controller.

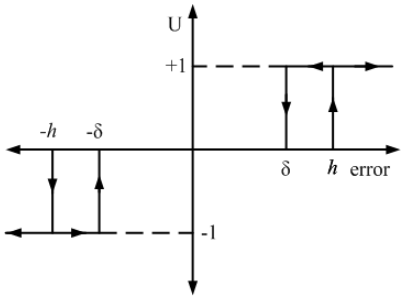

Fig. 2: Three-Level Hysteresis Switching Scheme

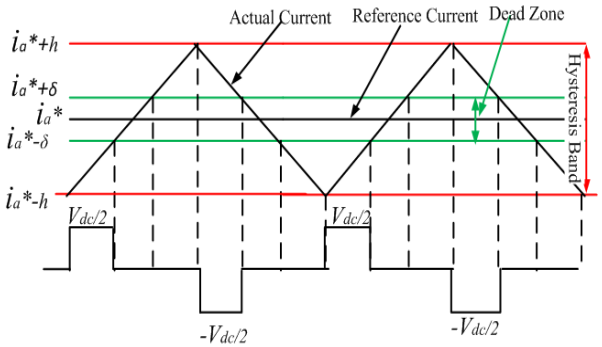

Fig. 3: Three-Level Hysteresis Current Control

To develop a switching scheme for the three-level inverter, the zero voltage level should be applied only at appropriate instants. The switching logic must ensure that there is no successive transition between $V_{dc}/2$ and $-V_{dc}/2$ states, as this will increase the frequency of switching. A dead zone 'δ' is necessary in the hysteresis band *'h'*, to avoid switching

towards two-level scheme, because of finite sampling rate of error. Without the dead zone, when the error becomes zero and is not detected, the opposite polarity of forcing function follows, resulting in a two-level scheme. However, the introduction of dead zone increases the tracking error and has to be chosen to a minimum value, depending on the best sampling speed that can be achieved [14].

If U represents the input state to be applied, e represents error $(i_a^* - i_a)$ and ce represents the change in error the switching logic is governed by equation (12)

If $e > 0$ then

$U = 1$ *for* $e \geq h$

$U = 0$ *for* $e \leq \delta$

$U = 0$ *for* $\delta < e < h$ *and* $ce > 0$

$U = 1$ *for* $\delta < e < h$ *and* $ce < 0$

Else if $e < 0$ then

$U = -1$ *for* $e \leq -h$

$U = 0$ *for* $e \geq -\delta$

$U = 0$ *for* $-\delta < e < -h$ *and* $ce < 0$

$U = -1$ *for* $-\delta < e < -h$ *and* $ce > 0$ (12)

The above logic represented in Fig.2 and Fig.3, tracks reference current either in the lower band (through 0 and +1 states) or in the upper band (through 0 and -1 states). Here $U = 1$, means the switch state is $V_{dc}/2$; $U = 0$ means the switch state is 0; and $U = -1$, means the switch state is $-V_{dc}/2$. Similarly the *b*-phase and *c*-phase switching function for the three-phase voltage source inverter can be obtained.

D. Indirect Vector Control

The indirect vector control is a technique that controls the dynamic speed of Induction motor. Unlike direct vector control, in indirect vector control, the unit vectors are generated in an indirect manner.

Fig.4 is the phasor diagram that explains the fundamental principle of indirect vector control. The $d^s - q^s$ axes are fixed on the stator and $d^r - q^r$ axes are fixed on the rotor which rotates at a speed ω_r. Synchronously rotating axes $d^e - q^e$ are rotating ahead of $d^r - q^r$ axes by the positive slip angle θ_{sl} corresponding to slip frequency ω_{sl}. Thus

$$\theta_e = \int \omega_e dt = \int (\omega_r + \omega_{sl}) dt \tag{13}$$

For decoupling control $\lambda_{qr} = 0$ or $p\lambda_{qr} = 0$ and $\lambda_r = \lambda_{dr}$. Substituting the above condition in equations (3), (4), (7) and (8)

$$\omega_{sl} = \frac{R_r L_m i_{qs}^e}{L_r \lambda_r} \tag{14}$$

$$T_e = \frac{3}{2}\frac{P}{2}\frac{L_m}{L_r}\lambda_r i_{qs}^e \tag{15}$$

$$i_{qs}^e = \frac{2}{3}\frac{2}{P}\frac{L_r}{L_m}\frac{T_e}{\lambda_r} \tag{16}$$

$$i_{ds}^e = \frac{1}{L_m}[\lambda_r + \frac{L_r}{R_r} p\lambda_r] \tag{17}$$

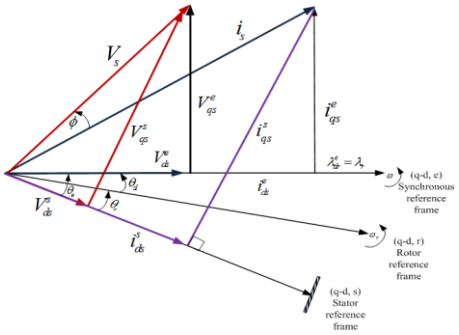

Fig. 4: Phasor diagram of Indirect Vector Control principle

III. ESTIMATION OF STATOR CURRENT SET POINT

The equations (14-17) are used to produce an adequate field orientation. These equations could be propagated to the set point variables [15].

$$\omega_{sl}^* = \frac{R_r L_m i_{qs}^{e^*}}{L_r \lambda_r^*} \tag{18}$$

$$i_{qs}^{e^*} = \frac{2}{3}\frac{2}{P}\frac{L_r}{L_m}\frac{T_e^*}{\lambda_r^*} \tag{19}$$

$$i_{ds}^{e^*} = \frac{1}{L_m}[\lambda_r^* + \frac{L_r}{R_r} p\lambda_r^*] \tag{20}$$

If it is accepted that the rotor flux set point is constant then its derivative is zero and the above equation is simplified as

$$i_{ds}^{e^*} = \frac{\lambda_r^*}{L_m} \tag{21}$$

Using the above equations the block diagram of indirect vector control of induction motor drive is as shown in Fig.5 [15].

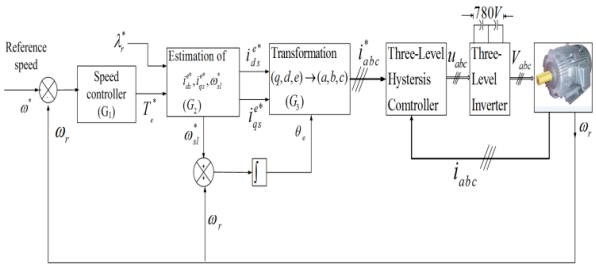

Fig. 5: Block diagram of Indirect Vector Control of IM

It contains three principal blocks. They are

G_1: Block of speed controller

G_2: Block of estimation of $i_{ds}^{e^*}$, $i_{qs}^{e^*}$ and ω_{sl}^*

G_3: Block of current co-ordinate transformation (q, d, e) to (a,b, c)

IV. PROPOSED SCHEME

A. *Block of speed controller*

The speed controller block G_1 is proposed to be a neuro-fuzzy controller (ANFIS) which incorporate fuzzy logic algorithm with a five layer artificial neural network structure [16], [17] .The speed error and the rate of change of actual speed error are the inputs of the neuro-fuzzy controller which determine the shape of each membership function and rules related to input- output variables in an optimized way from the data sets of inputs and output with the help of a training algorithm.

$$Input_1 = \varepsilon_\omega = \omega^* - \omega \tag{22}$$

$$Input_2 = \Delta\varepsilon_\omega = \varepsilon_\omega(n) - \varepsilon_\omega(n-1) \tag{23}$$

Where, ω is the actual speed and ω^* *is the command speed.*

First order Sugeno fuzzy model with five layers ANN structure is used in proposed controller [18], [19]. The proposed controller has two inputs with seven triangular membership functions each, one output with forty-nine linear membership functions and forty-nine rules as depicted in Fig.6. In proposed ANFIS controller, a hybrid learning algorithm is used which has two passes, forward and backward pass. In the forward pass, node output goes forward until layer-4 and the consequent parameters are identified by the sequential least square method. In backward pass, the error signal propagates backward and premise parameters are updated by gradient descent that is back propagation learning method [18], [19].

Fig.7 and Fig.8 shows output surface and input membership functions of proposed ANFIS respectively.

B. *Block of estimation of* $i_{ds}^{e^*}, i_{qs}^{e^*}$ *and* ω_{sl}^*

The block G_2 for the estimation of $i_{ds}^{e^*}, i_{qs}^{e^*}$ *and* ω_{sl}^* is realized by a feed forward neural network. The topology of the multi-layer feed forward network is of two input $\left(\lambda_r^*, T_e^*\right)$, three outputs $\left(i_{ds}^{e^*}, i_{qs}^{e^*} \text{ and } \omega_{sl}^*\right)$ and five and two neurons in the hidden layers (2-5-2-3). The offline algorithm of its learning is Levenberg-Marquardt. The final value of mean square error reached during the learning is 10^{-10}.

C. *Block of Current Co-Ordinate Transformation*

The block G_3 is realized by a feed forward neural network which performs a stator current set points (q-d, e) to (a,b,c) transformations. The topology of this multilayer feed forward network is of four inputs $\left(i_{ds}^{e^*}, i_{qs}^{e^*}, \sin\theta_e, \cos\theta_e\right)$, three outputs $\left(i_{as}^*, i_{bs}^*, i_{cs}^*\right)$ and two hidden layers of 20 and 10 neurons each (4-20-10-3). The off line algorithm of its learning is Levenberg-Marquardt. The final value of mean square error reached during the learning is 10^{-10}.

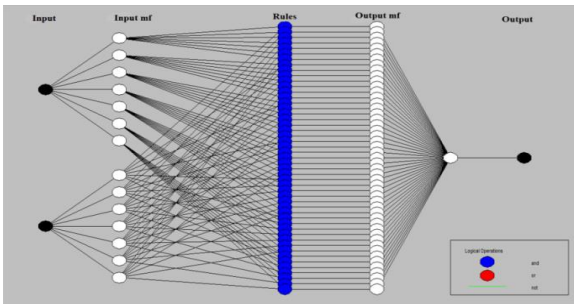

Fig. 6: Proposed ANFIS architecture

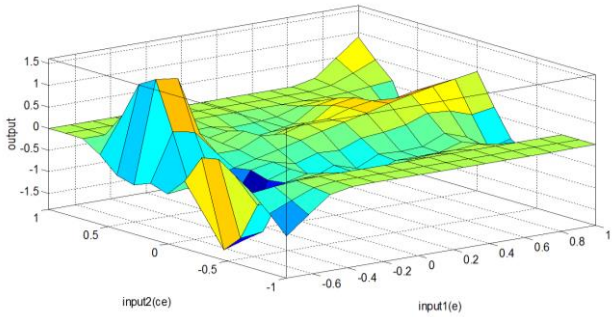

Fig. 7: Output surface of proposed ANFIS

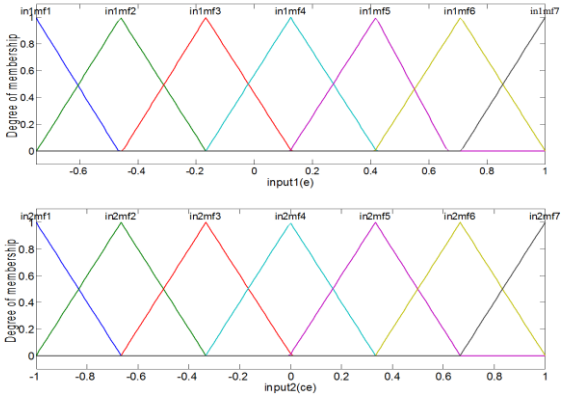

Fig. 8: Input membership function of proposed ANFIS

V. PERFORMANCE ASSESSMENT OF THE PROPOSED SCHEME

A complete simulation model for vector controlled Induction motor (IM) drive using the proposed scheme is developed. It is simulated with PI controller and required data for training the ANFIS controller is obtained. This paper uses the MATLAB ANFIS editor toolbox to train the ANFIS. The motor parameters are in Table II.

TABLE II: Induction Motor Parameters

Parameter	***Symbol***	***Value***
Rated Power	P_{rated}	50HP
Rated Voltage	*V*	480Volt
Rated Frequency	F	60Hz
Pair of poles	P	*2*
Stator Resistance	Rs	0:087
Rotor Resistance	Rr	0:228
Stator Inductance	Ls	0:8mH
Rotor Inductance	Lr	0:8mH
Mutual Inductance	Lm	34.7mH
Moment of Inertia	J	1.662Kg.m^2

Fig.9 shows the pole voltage, line voltage and the line currents (stator line currents) of the three-level inverter under steady state condition. The line currents are sinusoidal with almost negligible ripple.

Fig.10(a) and Fig.10(b) shows the speed tracking performance of the motor following a trapezoidal speed reference. The speed tracking experiment is on no load condition. The motor speed almost tracks the reference speed in both the direction but it contains ripple in torque at the time of speed change due to inertia of the motor.

Fig.11 shows the performance of motor for the constant reference speed of 120rad/sec with constant load torque 100Nm.The speed error is zero after the motor achieves the reference speed.

Fig.12 shows the performance of motor when the load torque is suddenly changed from 50Nm to 150Nm and then from 150Nm to 80Nm. The speed remains constant at reference speed 100rad/sec.

Fig.13 shows the performance of the motor when the reference speed is suddenly changed from 50rad/sec to 120rad/sec and then from 120rad/sec to 80rad/sec with a constant load torque of 100Nm.

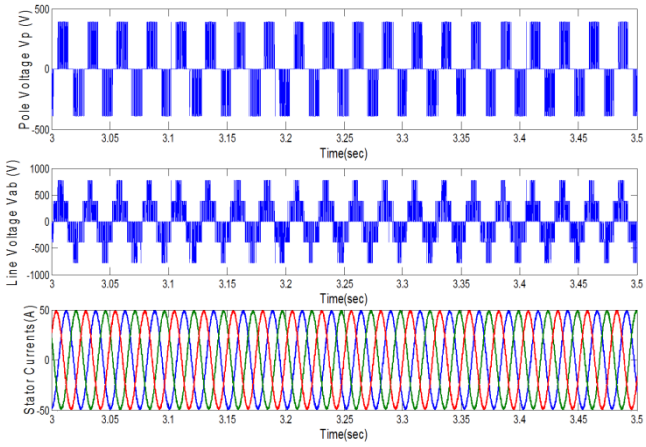

Fig. 9: Inverter Voltages and Currents

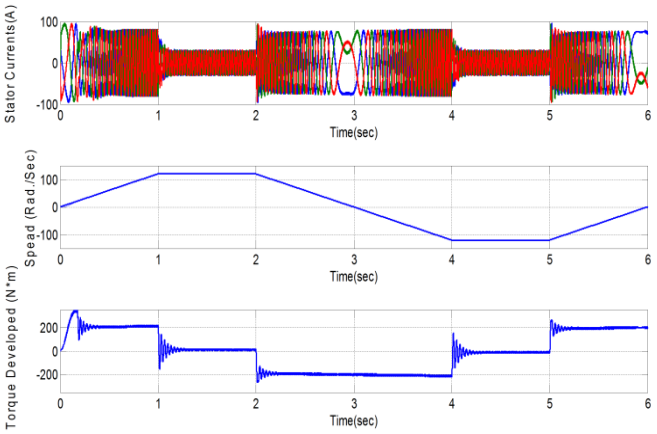

Fig. 10(a): Trapezoidal Speed Tracking

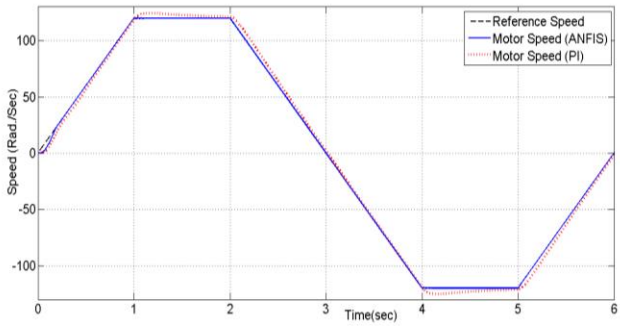

Fig. 10(b): Trapezoidal Speed Tracking of IM with ANFIS and PI controller

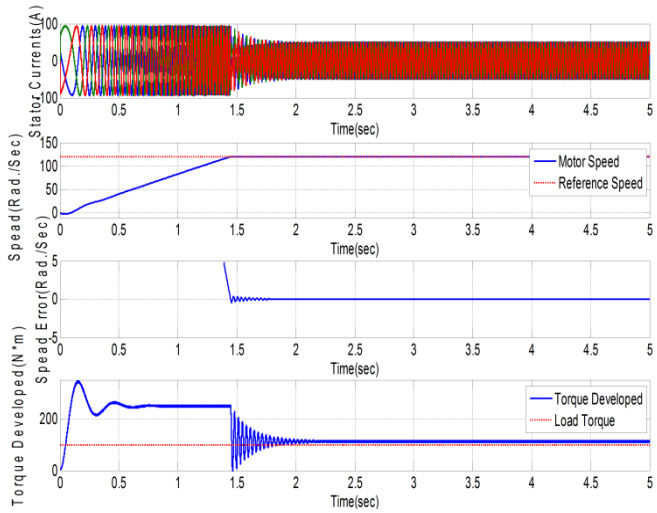

Fig. 11: Performance under constant speed and constant torque

Fig.14 shows the performance of the motor with variable speed and variable torque. The speed is increased from 50rad/sec to 120rad/sec and then decreased from 120rad/sec to 80rad/sec with a variable load torque. The load torque is increased from 30Nm to 150Nm and then it is decreased to 100 Nm.

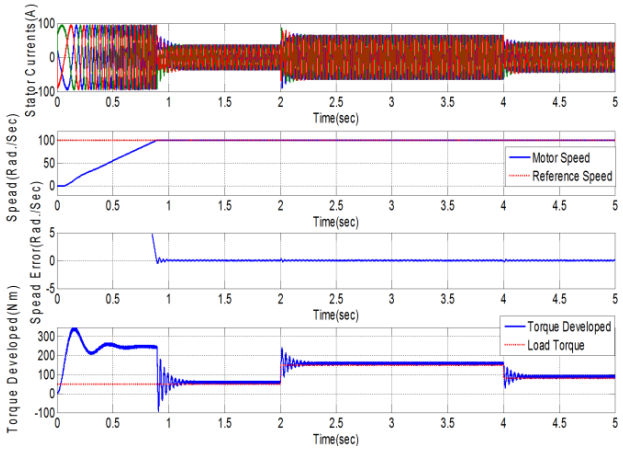

Fig. 12: Performance under constant speed and variable torque

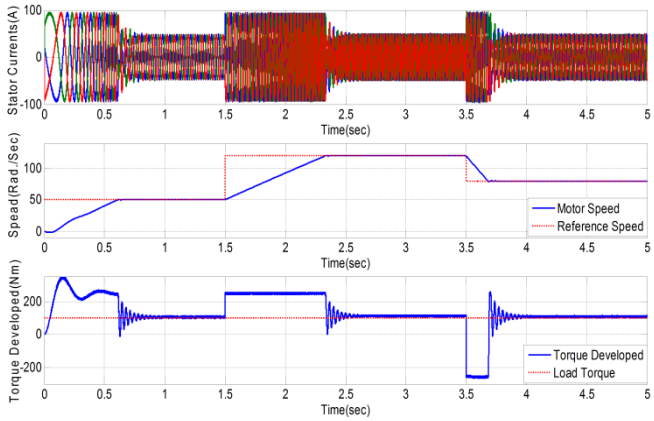

Fig. 13: Performance under variable speed and constant torque

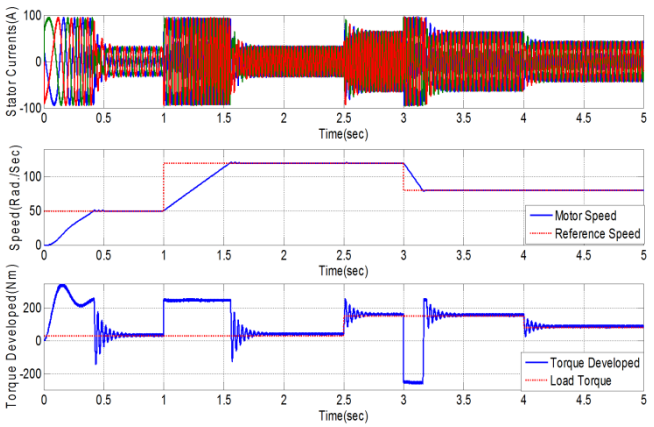

Fig. 14: Performance under variable speed and variable torque

VI. CONCLUSION

An indirect vector controlled multilevel fed induction motor drive is simulated with Neuro-fuzzy controller. The performance of drive is improved and due to the use of three level inverter, the current ripple and hence the torque ripple is reduced. Due to the use of Neuro-fuzzy controller the motor tracks the reference speed without any overshoot unlike PI controller.

To provide control action in ANFIS controller, only few rules have been used instead of all set of possible rules. Therefore, Genetic Algorithm (GA) can be utilized to train ANFIS controller in place of hybrid learning techniques. As well as GA can be used to obtain the optimal setting of input and output scaling factors of the controller. In hysteresis current controller switching frequency depends on selection of hysteresis band. This limitation can be overcome by space vector pulse width modulation (SVPWM).

REFERENCES

[1] B. K. Bose, Modern Power Electronics and AC Drives. Prentice-Hill PTR Companies, Inc. Upper Saddle River, NJ 07458, 2002.

[2] P. Vas, Vector control of AC machines. New York: Clarendon, 1990.

[3] R. Krishnan, Electric motor drives modeling, analysis and control. New Delhi: PHI Pvt. Ltd, 2003.

[4] A. Nabae, I. Takahasi, and H. Akagi, “A neutral point clamped pwm inverter.” IEEE Transaction on Industry Applications, vol. 1A, no. 17, pp. 518–523, Sept./Oct 1981.

[5] R. K. Behera and S. P. Das, “Three-level inverter-fed high performance induction motor drive system,” APSC-2004 NIT Rourkela, pp. 45–50,November 2004.

[6] J.-S. L. Jos Rodrguez and F. Z. Peng, “Multilevel inverters: A survey of topologies, controls, and applications,” IEEE Transaction on Industrial Electronics, vol. 49, no. 4, August 2002.

[7] X. Yuan and I. Barbi, “A new diode clamping multilevel inverter,” IEEE, conference, pp. 495–501, 1999.

[8] T. V. Dixit, R. K. Behera, and S. P. Das, “Design of high power three-level utility friendly converter for power quality applications,” IEEE conference (PSACO-08), Andhra University, Visakhapatnam, India, pp. 413–419, March 13-15 2008.

[9] R. K.Behera, T. V. Dixit, and S. P. Das, “Analysis of experimental investigation of various carrier-based modulation schemes for three-level neutral point clamped inverter-fed induction motor drive,” IEEE conf (PEDES06), Delhi, India, pp. 1–6, December 12-15 2006.

[10] R. K. Behera, T. Dixit, and S. P. Das, “Describing function analysis and experimental investigation of a high power utility friendly ac-dc converter system,” in Proceedings of IEEE-IECON 06, November 7-10, 2006, p. 2186 219

[11] M. Kazmierkowski and L. Malesani, “Current control techniques for three-phase voltage-source pwm converters: A survey,” IEEE Transaction Ind. Electron, vol. 45, no. 5, pp. 691–703, 1998.

[12] J. Zeng, C. Yu., Q. Qi., Z. Yan., Y. Ni., B. Zhang, S. Chen, and F. F. Wu., “A novel hysteresis current control for active power filter with constant frequency,” Electric Power Systems Research, vol. 68, pp. 75–82, 2004.

[13] M. Milosevic, “Hysteresis current control in three-phase voltage source inverter,” Technical Report, Zurich, 2003.

[14] S. Srikanthan, M. Mishra, and R. Rao, “Improved hysteresis current control of three-level inverter for distribution static compensator application.”IET Power Electronics, vol. 2, no. 5, pp. 517–526, 2009.

[15] S. K. Sahu, D. D. Neema, and T. V. Dixit, “Indirect vector control of induction motor using ann estimator and ANFIS controller,” International Journal of Computer Applications, vol. 66, no. 14, March 2013.

[16] M. Aware, A. Kothari, and S. Choube, “Application of adaptive neuro-fuzzy controller (anfis) for voltage source inverter fed induction motor drive,” in Proc. of IPEMC Conf, vol. 2, 15-18 Aug,2000, pp. 935–939.

[17] P. P. Cruz, J. M. Aquino, and M. R. Elizondo, “Vector control using ANFIS controller with space vector modulation [induction motor drive application],” in Proc. of UPEC Conf., vol. 2, 6-8 Sept. 2004, pp. 545–549.

[18] J. Jang, C. Sun, and E. Mizutani, Neuro-Fuzzy and soft computing- A computational approach to learning and machine intelligence. PHI Pvt. Ltd., New Delhi, 2006.

[19] R. Kumar, R. A. Gupta, and R. S. Surjuse, “Adaptive neuro-fuzzy speed controller for vector controlled induction motor drive,” Asian Power Electronics Journal, vol. 03, no. 1, pp. 8–14, Sept 2009.